



HAL
open science

A complete solid solution between GeO₂ and SiO₂ with the α -quartz structure: additional X-ray diffraction data from Ge_{1-x}Si_xO₂ flux-grown crystals

Pascale Armand, Dominique Granier, Monique Tillard

► To cite this version:

Pascale Armand, Dominique Granier, Monique Tillard. A complete solid solution between GeO₂ and SiO₂ with the α -quartz structure: additional X-ray diffraction data from Ge_{1-x}Si_xO₂ flux-grown crystals. *Journal of Solid State Chemistry*, 2023, 317, pp.123658. 10.1016/j.jssc.2022.123658. hal-03830205

HAL Id: hal-03830205

<https://hal.science/hal-03830205>

Submitted on 26 Oct 2022

HAL is a multi-disciplinary open access archive for the deposit and dissemination of scientific research documents, whether they are published or not. The documents may come from teaching and research institutions in France or abroad, or from public or private research centers.

L'archive ouverte pluridisciplinaire **HAL**, est destinée au dépôt et à la diffusion de documents scientifiques de niveau recherche, publiés ou non, émanant des établissements d'enseignement et de recherche français ou étrangers, des laboratoires publics ou privés.

A complete solid solution between GeO_2 and SiO_2 with the α -quartz structure:
additional X-ray diffraction data from $\text{Ge}_{1-x}\text{Si}_x\text{O}_2$ flux-grown crystals.

Pascale Armand *, Dominique Granier, Monique Tillard

ICGM, Univ Montpellier, CNRS, ENSCM, Montpellier, France

*Corresponding author: pascale.armand@umontpellier.fr

ORCID: P. Armand 0000-0001-8921-5427

M. Tillard 0000-0002-0609-7224

Keywords: α -Quartz structure; GeO_2 ; X-ray diffraction; SiO_2 .

Abstract

Millimeter-sized crystals of formula $\text{Ge}_{1-x}\text{Si}_x\text{O}_2$, *i.e.* GeO_2 materials partially substituted by SiO_2 , were obtained for the first time both in the middle and the Si-rich parts of the GeO_2 – SiO_2 composition domain ($0.5 \leq x \leq 0.93$) by spontaneous nucleation using the high-temperature flux method. The X-ray crystal diffraction (XRD) data at room temperature confirm the non-centrosymmetric α -quartz-type structure and the low level of defects for these as-grown materials. The silicon content in the $\text{Ge}_{1-x}\text{Si}_x\text{O}_2$ crystals was determined by interpolation from the inter-tetrahedral bridging angle. The complete mutual solubility is confirmed between α - SiO_2 and α - GeO_2 . The deviation from the regularity of the TO_4 tetrahedra ($T = \text{Si}, \text{Ge}$) decreases linearly when Ge is gradually replaced by Si.

I. Introduction

The quartz-alpha SiO_2 ($P3_121$ or $P3_221$ space group), with its very precise and very stable oscillation frequencies, is one of the most widely used piezoelectric crystals in the electronics industry for applications as oscillators or in the time-frequency domain. The control of its hydrothermal growth process makes it possible to obtain large and high-quality crystals for industrial uses. However, quartz has a low electromechanical coupling factor k_{11} of about 9%, and upon heating, it shows a decrease in its properties above 350°C mainly due to an alpha-beta quartz phase transition at 573°C [1-3]. To overcome the weakness of quartz in terms of k and thermal stability, α -quartz-like materials such as GeO_2 and MXO_4 compounds ($M = \text{B, Al, Ga, Fe, Mn}$; $X = \text{P, As}$) have also been studied [4, 5].

Flux-grown germanium dioxide with the α -quartz structure ($\alpha\text{-GeO}_2$) has a wide operating temperature range under atmospheric pressure until it melts at 1115°C [6]. At room temperature, this material is largely more efficient than quartz with 3 times higher piezoelectric coefficients [7]. In addition, piezoelectric properties are preserved when the $\alpha\text{-GeO}_2$ material is subjected to very high temperatures [7, 8]. The strong structural distortion and the meta-stability of the α -quartz structure of GeO_2 make it difficult to hydrothermally grow it as large OH-free single crystals OH-free large single-crystals [9]. The high-temperature flux technique has been used successfully to grow $\alpha\text{-GeO}_2$ single-crystals with high crystalline quality [10]. Nevertheless, there is no industrial production by seeded solution growths of large $\alpha\text{-GeO}_2$ crystals.

The existence of a solid solution between two pure compounds offers the possibility to adjust the physical properties by adapting the chemical compositions. Several flux-grown mixed compositions are reported in the GeO_2 -rich part of the $\text{GeO}_2\text{-SiO}_2$ binary diagram with the low-temperature α -quartz phase [11, 12]. In addition, non-centrosymmetric mixed crystals

grown hydrothermally have been described in the SiO₂-rich part [13-15]. Therefore, until now, the growth of α -quartz-type single crystals with a SiO₂ content between 20 and 80 mol.% has never been reported in the GeO₂-SiO₂ solid solution.

In the absence of postponed compositions in the middle part of the GeO₂-SiO₂ binary, a second-order polynomial was used in [11] to fit the evolution with the chemical composition of the ambient lattice parameters a and c . Thus, to validate this deviation from Vegard's law, compositions needed to be reported in the middle part of the GeO₂-SiO₂ binary diagram. The high-temperature flux technique with the spontaneous nucleation method was used in the current work to obtain new mixed Ge_{1-x}Si_xO₂ single-crystals with $0.5 \leq x \leq 0.93$ and consequently to validate the complete mutual solubility which exists between α -SiO₂ and α -GeO₂.

In this paper, we report the structural results obtained for four crystal compositions from X-ray diffraction (XRD) measurements at room temperature. The effects of the germanium substitution by silicon on the α -quartz type structure are followed through the variation of structural parameters and angular distortions.

II. Experimental section

Synthesis

Mixed SiO₂-GeO₂ single-crystals were grown by spontaneous nucleation in K₂Mo₃O₁₀ flux with the use of the slow-cooling growth process. The high-temperature flux method used for growth experiments has already been described in detail elsewhere [12]. In a first step, solutes with 3 different GeO₂/SiO₂ mole ratios of 1, 0.66, and 0.11 were prepared by heating high purity commercial GeO₂ and SiO₂ powders (99.999% AlfaAesar products) at a very high temperature ($T > 1400^\circ\text{C}$) and then air quenching. Then "solute/flux (K₂Mo₃O₁₀)" mixtures

were prepared with a weight ratio of 10 / 90 whatever the solute composition. For each flux-growth experiment, the 15g-powdered mixture was placed in a Pt crucible covered with a lid, then heated up (150°C/h) to 1020°C, held at this temperature for 24h, then slowly cooled down (5°C/h) to 650°C before turning off the furnace.

For each growth performed in this work, several millimeter-sized transparent and colorless crystals were found trapped in the solidified flux after cooling to room temperature. The crystals were separated from the flux by dissolving the flux in water and they were washed several times with deionized water before their characterization. The reaction yields were of the order of 8 - 10 %.

X-ray diffraction

An Xcalibur four-circle diffractometer (Oxford diffraction) equipped with both a molybdenum anticathode (monochromatic Mo K α radiation, $\lambda = 0.71073\text{\AA}$) and a CCD detector was used to perform XRD experiments at ambient conditions. As-grown crystals from each experiment were selected by using a stereo microscope equipped with a polarizing filter. Diffraction experiments were performed at room temperature for the best suitable crystals expected to be single crystals. The appropriate software suite CrysAlis [16] was used to handle the collected data and to apply the Lorentz-polarization and absorption corrections to the diffracted intensities.

Structural full-matrix least-squares refinements on F^2 were performed using the SHELX programs [17, 18]. Atomic form factors of neutral atoms extracted from the International Tables for Crystallography were used [19]. Refinements were performed in the trigonal space group $P3_121$ (n°152) with an atomic Ge/Si mixture at a $3a$ special site and an oxygen atom at a general site $6c$. Anisotropic displacement parameters were considered for all atoms. The resulting atomic positions were standardized using the Structure Tidy program [20].

III. Results and discussion

The transparent flux-grown mixed $\text{Ge}_{1-x}\text{Si}_x\text{O}_2$ materials with $0.5 \leq x \leq 0.93$ were obtained as individualized colorless crystals. Since these materials result from the partial replacement of germanium by silicon at the same position in the structure, it follows obviously that an increase in their Si content corresponds to a decrease in their Ge content. Four crystals in total were selected for the current diffraction study, one from each of the growth experiments carried out with $\text{GeO}_2/\text{SiO}_2$ molar ratios of 1 and 0.11 and additionally, two coming from the same experiment with a $\text{GeO}_2/\text{SiO}_2$ molar ratio of 0.66. This latter choice was intentional to check the homogeneity in composition and the crystalline quality within the material spontaneously grown as crystals. The main information about data collection is provided below in Table I.

The recorded data display the trigonal symmetry which confirms the crystallization of the studied samples with the α -quartz-type structure. The unit cell contains three units of the formula $\text{Ge}_{1-x}\text{Si}_x\text{O}_2$ ($Z = 3$). After careful examination of their diffraction data, three crystals were suspected to be twinned and the corresponding refinements were therefore carried out using TWIN and BASF instructions, which led to a marked improvement in the refinement behavior with a significant decrease in the final agreement factors. The full CIF files are freely available by providing the CSD numbers 2192926 ($\text{Ge}_{0.07}\text{Si}_{0.93}\text{O}_2$), 2192927 ($\text{Ge}_{0.37}\text{Si}_{0.63}\text{O}_2$), 2192928 ($\text{Ge}_{0.52}\text{Si}_{0.48}\text{O}_2$), 2193019 ($\text{Ge}_{0.39}\text{Si}_{0.61}\text{O}_2$) at the Cambridge Crystallographic Data Center [21].

Due to the very small sizes of the crystals, it was not possible to obtain reliable chemical analyses for those selected and used in the diffraction experiments. Alternatively, as already demonstrated in [11], some geometry parameters are useful to estimate with rather good precision the composition of $\text{Ge}_{1-x}\text{Si}_x\text{O}_2$ samples having trigonal α -quartz structures. This is particularly the case of the inter-tetrahedral $T\text{-O-T}$ angle ($T = \text{Si}, \text{Ge}$) found to vary linearly

with the Si content (x value) [11]. Note that the Si content is always represented by x in the formulas but it is also reported in the following as x_{Si} , particularly in figures and equations. The bridging angle $T\text{--O--}T$ is the angle formed between two TO_4 tetrahedral vertex-sharing units. This angular parameter does not depend on the Ge to Si ratio but is determined only by the relative position of the peaks (associated with atomic positions) in the electronic density map. According to our previous results [9], the inter tetrahedral $T\text{--O--}T$ angle, measured at 130.140° for $\alpha\text{-GeO}_2$ and 143.625° for $\alpha\text{-SiO}_2$, is assumed to have a linear variation over the entire composition domain in the $\alpha\text{-GeO}_2\text{--}\alpha\text{-SiO}_2$ pseudo-binary system. Its variation was found to follow the relation:

$$T\text{--O--}T (\text{°}) = 13.540 \times x_{\text{Si}} + 130.17 \quad (1)$$

Ge_{1-x}Si_xO₂ formula	Ge_{0.52}Si_{0.48}O₂	Ge_{0.39}Si_{0.61}O₂	Ge_{0.37}Si_{0.63}O₂	Ge_{0.07}Si_{0.93}O₂
Si content, x_{Si}	0.48	0.61	0.63	0.93
Formula weight, g.mol⁻¹	83.23	77.44	76.56	63.21
Space group	$P3_121$ (n°152)	$P3_121$ (n°152)	$P3_121$ (n°152)	$P3_121$ (n°152)
Cell dimensions $a, c, \text{Å}$	4.9541(2) 5.5032(3)	4.9451(1) 5.4789(1)	4.9444(2) 5.4754(3)	4.9293(1) 5.4224(1)
c/a	1.111	1.107	1.107	1.100
Cell volume, Å³	116.969(10)	116.030(5)	115.924(11)	114.106(5)
$T\text{--O--}T$ angle, °	136.7(3)	138.7(1)	138.8(1)	142.7(1)
d_{calc}, g.cm⁻³	3.545	3.325	3.290	2.759
F(000)	118	111	110	94
Abs. coef. μ, mm⁻¹	10.39	8.10	7.74	2.29
Transmission factors	0.32–0.65	0.20–0.37	0.61–0.80	0.74–0.77
Crystal size, μm	82×91×183	46×52×107	46×59×93	84×98×108
θ range, °	4.75 – 32.67	3.72 – 32.31	3.72 – 32.30	3.76 – 32.46
Collected/ unique refls	4457 / 277	4514 / 276	4473 / 275	5906 / 273

R_{int}	0.0697	0.0215	0.0365	0.0247
$R1 [I > 2\sigma(I)]$	0.0233	0.0101	0.0135	0.0094
$wR_2 [I > 2\sigma(I)]$	0.0622	0.0299	0.0323	0.0242
S	1.348	1.281	1.320	1.207
Extinction coef.	0.034(1)	-	-	0.11(2)
Flack coef.	0.01(5)	-0.007(13)	0.001(17)	0.01(3)
$\Delta\rho$ residuals, $e.\text{\AA}^{-3}$	0.40 / -0.49	0.29 / -0.35	0.45 / -0.53	0.16 / -0.16
r.m.s. deviation $e.\text{\AA}^{-3}$	0.121	0.075	0.122	0.046

Table I: Main crystal data and structural parameters at room temperature for $\text{Ge}_{1-x}\text{Si}_x\text{O}_2$ crystals ($T = \text{Si, Ge}$). $R_{int} = \Sigma|F_o^2 - \langle F_o^2 \rangle| / \Sigma F_o^2$, $R1 = \Sigma||F_o| - |F_c|| / \Sigma|F_o|$, $wR_2 = [\Sigma w(F_o^2 - F_c^2)^2 / \Sigma w(F_o^2)^2]^{1/2}$ and, $S = \text{G.O.F.} = [\Sigma w(F_o^2 - F_c^2)^2 / (n-p)]^{1/2}$ for n reflections and p refined parameters

In the current study, the XRD data processing was performed in two steps according to the procedure already used for flux-growing $\alpha\text{-Ge}_{1-x}\text{Si}_x\text{O}_2$ single crystals with $0.021 \leq x \leq 0.18$ in the previous work [11]. So, for each crystal under study, we performed first a series of structural refinements in which the Ge/Si ratio could vary freely. Since Ge and Si are mixed at the same atomic position, the sum of Ge and Si contents is necessarily kept equal to 1 (full site occupation).

The value of the inter-tetrahedral angle $T\text{-O-T}$ which is obtained in such refinement was then used to estimate the Si-content (x_{Si}) in the as-grown $\alpha\text{-Ge}_{1-x}\text{Si}_x\text{O}_2$ crystal. Then, the Ge and Si contents were fixed at their estimated values in a new series of refinements. At the end of each structural refinement, it should be noted that the new $T\text{-O-T}$ angular value does not significantly differ (within the 3σ limits) from that formerly used for the evaluation of the chemical composition.

Two $\text{Ge}_{1-x}\text{Si}_x\text{O}_2$ samples ($x = 0.61$ and 0.63) coming from the same growth experiment with a $\text{GeO}_2/\text{SiO}_2$ molar ratio solute of 0.66 were characterized to check how similar are the Ge/Si ratios in crystals from a same reaction. From the two crystals under study ($\text{Ge}_{0.39}\text{Si}_{0.61}\text{O}_2$ and $\text{Ge}_{0.37}\text{Si}_{0.63}\text{O}_2$), the Ge/Si ratio distribution was found close to 5% regarding the accuracy of the method for the chemical determination.

The crystal data and refinement main parameters are reported in Table I for $\text{Ge}_{1-x}\text{Si}_x\text{O}_2$ samples with $x = 0.48, 0.61, 0.63, 0.93$. The final agreement factors R1, wR2, and S assess the good quality of the structures. The Flack coefficients, which are absolute structure parameters, are refined to values close to zero providing information on the absence of crystalline parts corresponding to the inverse structural model. The atomic fractional coordinates are given in Table II with the equivalent isotropic displacement parameters. The current oxygen coordinates must be transformed by applying the symmetry operation $(-x, y-x, 1/3-z)$ for direct comparison with positions reported in [11].

$\text{Ge}_{1-x}\text{Si}_x\text{O}_2$ formula	$\text{Ge}_{0.52}\text{Si}_{0.48}\text{O}_2$	$\text{Ge}_{0.39}\text{Si}_{0.61}\text{O}_2$	$\text{Ge}_{0.37}\text{Si}_{0.63}\text{O}_2$	$\text{Ge}_{0.07}\text{Si}_{0.93}\text{O}_2$
Si content, x_{Si}	0.48	0.61	0.63	0.93
$T(x_T, 0, \frac{1}{3})$	0.4583(2)	0.46075(9)	0.46079(11)	0.46749(8)
$U_{\text{eq } T} (\times 100, \text{\AA}^2)$	0.136(3)	0.907(11)	0.945(12)	0.769(11)
x_{O}	0.4051(9)	0.4086(4)	0.4088(5)	0.4124(3)
y_{O}	0.2852(9)	0.2814(4)	0.2811(4)	0.2700(2)
z_{O}	0.2294(6)	0.2261(3)	0.1075(3)	0.2169(2)
$U_{\text{eq } \text{O}} (\times 100, \text{\AA}^2)$	2.09(7)	1.71(3)	1.80(3)	1.60(2)

Table II: Fractional coordinates and equivalent isotropic displacement parameters U_{eq} in $\text{Ge}_{1-x}\text{Si}_x\text{O}_2$. Atoms $T = \text{Si/Ge}$ are placed at $3a$ special position $(x_T, 0, \frac{1}{3})$ and O at $6c$ general position $(x_{\text{O}}, y_{\text{O}}, z_{\text{O}})$.

In the work earlier reported by Lignie et al. [11] for the trigonal $\alpha\text{-Ge}_{1-x}\text{Si}_x\text{O}_2$ compositions, data was missing in the middle part of the $\alpha\text{-GeO}_2\text{-}\alpha\text{-SiO}_2$ pseudo-binary system. The new flux-growth syntheses in this solid solution domain have yielded high-quality crystals characterized in the current work by non-centrosymmetric trigonal symmetry. Consequently, new crystallographic data are now available (Table I) to complete the sampling in the solid solution $\alpha\text{-GeO}_2\text{-}\alpha\text{-SiO}_2$ and provide for the first time real proof of the continuity of this solid solution over its entire composition domain.

The evolution of both the experimental lattice parameters at room temperature and the c/a ratio is plotted as a function of the Si-content x_{Si} in Figure 1. The ambient cell parameters for the terminal members, $\alpha\text{-GeO}_2$ and $\alpha\text{-SiO}_2$ are taken from the previous work, as well as for the GeO_2 -rich flux-grown $\alpha\text{-Ge}_{1-x}\text{Si}_x\text{O}_2$ compositions with $0.021 \leq x \leq 0.18$, [11].

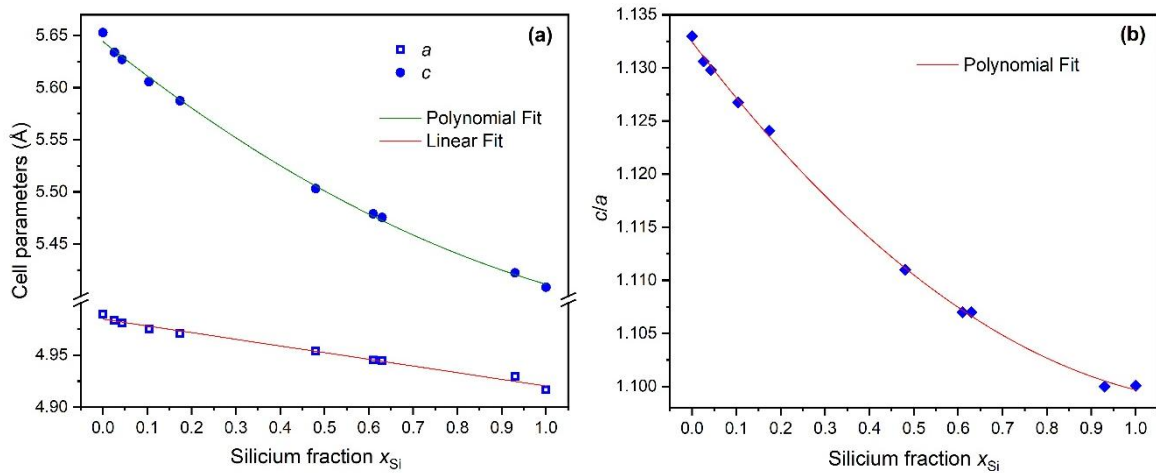


Figure 1: Evolution of (a) unit cell parameters a and c and (b) c/a ratio with the silicon content in $\alpha\text{-Ge}_{1-x}\text{Si}_x\text{O}_2$. Solid lines are fitting curves of the experimental data. Error bars are smaller than the symbol size. Data for $x_{\text{Si}} = 0, 0.026, 0.043, 0.104, 0.174, 1$ are taken from [11].

As the substitution of Ge by Si increases, the cell parameters a , c , and the c/a ratio are found to decrease, which corresponds to a reduction in the cell volume, Table I and Fig. 1. The

progressive replacement in the structure of $\alpha\text{-Ge}_{1-x}\text{Si}_x\text{O}_2$ of the Ge atoms by Si atoms affects the lattice constants and it is not unexpected as Si is a smaller element than Ge. As these elements are present as cations in this structure, it is relevant to compare their ionic radii and to observe that the ionic radius of Si^{4+} is about 32% smaller than that of Ge^{4+} .

Over the whole $\text{GeO}_2\text{-SiO}_2$ solid solution range, the behavior of parameter c was fitted to a second-degree polynomial, Fig. 1(a). When considering a second-order polynomial fit for parameter a , the second-order term is found extremely small and therefore the linear fit given below is more relevant.

$$a \text{ (\AA)} = -0.064 \times x_{\text{Si}} + 4.980 \quad (2)$$

$$c \text{ (\AA)} = 0.107 \times x_{\text{Si}}^2 - 0.341 \times x_{\text{Si}} + 5.640 \quad (3)$$

A second-order polynomial was the best to fit the behavior of the c/a value as a function of the Si content in the $\text{GeO}_2\text{-SiO}_2$ system, Fig. 1(b):

$$c/a = 0.022 \times x_{\text{Si}}^2 - 0.055 \times x_{\text{Si}} + 1.133 \quad (4)$$

The c parameter and therefore the c/a ratio for crystals with the α -quartz structure in the $\text{GeO}_2\text{-SiO}_2$ pseudo-binary system does not follow Vegard's law (Fig. 1). The deviation from Vegard's law for these two parameters was already reported in a previous paper where both the a and c experimental cell parameters were fitted with a second-order polynomial [11]. The addition of new data for some compositions $\alpha\text{-Ge}_{1-x}\text{Si}_x\text{O}_2$ in the middle range, now, permits consideration of a linear variation with the Si-content for the parameter a in the solid solution $\text{GeO}_2\text{-SiO}_2$. In contrast, the variation of parameter c is still well-fitted with a second-order polynomial. Based on the present characteristics, it is confirmed that the volume contraction

with increasing the Si fraction occurs preferentially along the polar c -axis, as stated earlier [11].

Also interesting are the variations with the Si content of the inter-atomic distances $T-O$ and the intra-tetrahedral angles $O-T-O$ ($T = \text{Si, Ge}$). As there are four $T-O$ bonds in a tetrahedron, there are therefore 6 intra-tetrahedral angles. These bond lengths and angular values are listed in Table III for the four Si/Ge mixed compositions under study. The $T-O$ bond length decreases as the Si content increases in good agreement with the drastic reduction in the ionic radius (also atomic radius decrease) when going from Ge to Si. This is well illustrated in Figure 2 with the variation of the average bond lengths values $\langle T-O \rangle$ drawn as a function of the Si content, x_{Si} , for various compositions of the germanium-silicon oxides $\alpha\text{-Ge}_{1-x}\text{Si}_x\text{O}_2$.

Ge_{1-x}Si_xO₂ formula	Ge_{0.52}Si_{0.48}O₂	Ge_{0.39}Si_{0.61}O₂	Ge_{0.37}Si_{0.63}O₂	Ge_{0.07}Si_{0.93}O₂
Si content, x_{Si}	0.48	0.61	0.63	0.93
$T-O$ bond	$2 \times 1.663(4)$ $2 \times 1.675(3)$	$2 \times 1.645(2)$ $2 \times 1.660(2)$	$2 \times 1.644(2)$ $2 \times 1.658(2)$	$2 \times 1.614(1)$ $2 \times 1.626(1)$
$\langle T-O \rangle$ mean bond	1.6692	1.6525	1.6511	1.6197
d.i. (T-O)	0.0019	0.0022	0.0022	0.0018
O-T-O angles	107.8(1) 107.8(1) 108.6(3) 108.9(3) 111.9(2) 111.9(2)	108.0(1) 108.0(1) 109.1(1) 109.3(1) 111.2(1) 111.2(1)	108.1(1) 108.1(1) 109.2(1) 109.2(1) 111.2(1) 111.2(1)	108.7(1) 108.7(1) 109.0(1) 109.1(1) 110.6(1) 110.6(1)
$\langle O-T-O \rangle$ mean angle	109.48	109.46	109.48	109.48

$d.i. (O-T-O)$	0.0145	0.0107	0.0103	0.0071
----------------	--------	--------	--------	--------

Table III: $T-O$ bond lengths (\AA) and $O-T-O$ intra-tetrahedron angles ($^\circ$) ($T = \text{Si, Ge}$). The associated distortion indices are defined as $d.i. = \sum_{i=1}^n |y_i - \langle y \rangle| / (n \times \langle y \rangle)$ where y_i and $\langle y \rangle$ are the individual and average values of tetrahedral bond lengths or intra-tetrahedral angles [11]. Standard deviations are given in parentheses.

A second-order polynomial fit of the $\langle T-O \rangle$ experimental average values $\langle T-O \rangle$ gives the following equation:

$$\langle T-O \rangle (\text{\AA}) = 0.032 \times x_{\text{Si}}^2 - 0.158 \times x_{\text{Si}} + 1.737 \quad (5)$$

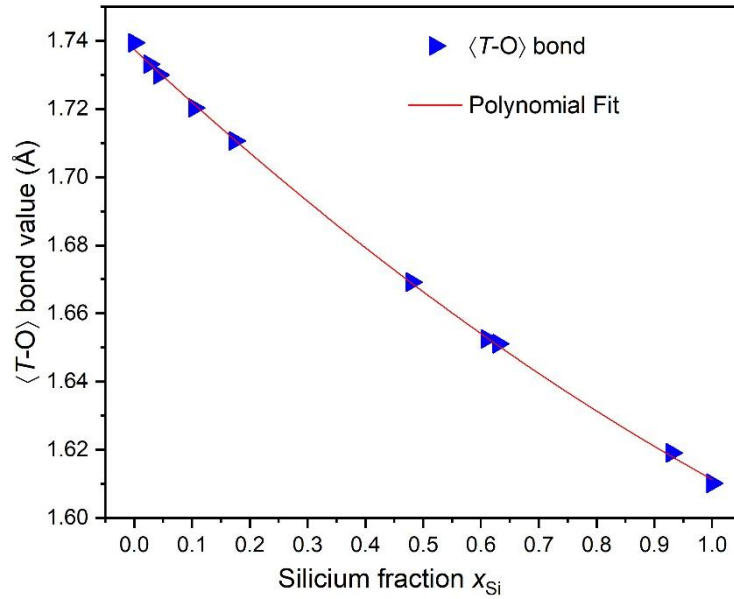


Figure 2: Evolution of $\langle T-O \rangle$, the average value of $T-O$ bond lengths, with the Si content. Data for $x_{\text{Si}} = 0, 0.026, 0.043, 0.104, 0.174, 1$ are taken from [11]. Solid line represents the second-order least squares fit. The error bars are smaller than the symbol size.

To follow the structural changes along with the substitution rate, it is instructive to look at the distortion indices calculated for the $T-O$ bond lengths and for the $O-T-O$ intra-tetrahedral angles. The distortion index is a parameter that gives an evaluation of the deviation of

individual parameters to their mean value. Note that only slight changes occur in the distortion indices (*d.i.*) corresponding to the T -O distances in TO_4 tetrahedra when passing from α -GeO₂ to α -SiO₂. This indicates that changing the nature of the T atom does not produce bond length dispersion in the tetrahedra TO_4 , which is normal as only one crystallographic site is concerned and substitution is done homogeneously at all the tetrahedron vertices such as the four bond lengths vary together.

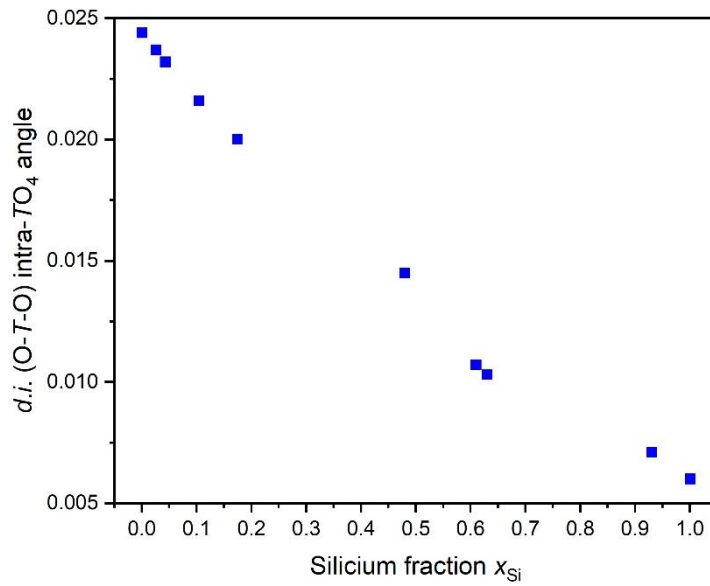


Figure 3: Evolution of the distortion indices for intra-tetrahedral O-T-O angles with the Si-content. Data for $x_{Si} = 0, 0.026, 0.043, 0.104, 0.174, 1$ are taken from [11]. Error bars are smaller than the symbol size. Distortion indices are defined as $(\sum_{i=1}^n |y_i - \langle y \rangle|) / (n * \langle y \rangle)$ with y_i the individual and $\langle y \rangle$ the mean intra-tetrahedral angles [9].

Instead, a great decrease is noted for the intra-tetrahedral angular distortion indices *d.i.* (O-T-O) as reported in Table III and Fig. 3. This parameter is representative of the O-T-O angles ability to approach the ideal value of 109.5° which is characteristic of a regular tetrahedron. Its variation brings a good image of the trend for the TO_4 tetrahedra described in the $P3_121$ space group with symmetry 3 to gradually approach the symmetry T_d as the Si content increases.

In the TO_2 family ($T = \text{Si}, \text{Ge}$), the α -quartz-type trigonal structure is composed of TO_4 tetrahedra, each sharing two vertices with alike units. Thus, variations in the intra-tetrahedral angles also result in correlated changes in the inter-tetrahedral bridging angles $T-O-T$. The reduction of the TO_4 tetrahedra distortion, associated with the diminution of *d.i.* ($O-T-O$) when the Si content increases in these mixed-growth compounds, Fig. 3, marks the tendency for the TO_4 units to approach the tetrahedral symmetry. This is made possible by the simultaneous decrease in the $O-T-O$ intra-tetrahedral angles, Table III, and the c/a ratio, Fig. 1(b), along with the increase in the bridging $T-O-T$ angles, Fig. 4.

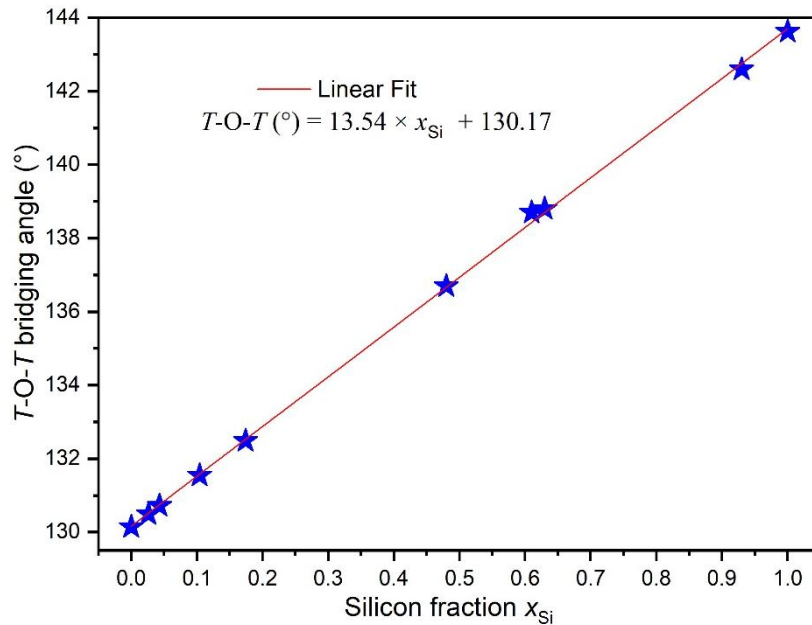


Figure 4: Evolution of the bridging $T-O-T$ angle between TO_4 units with the Si content. Data for $x_{\text{Si}} = 0, 0.026, 0.043, 0.104, 0.174, 1$ come from [11]. Error bars are smaller than the symbol size.

IV. Conclusion

In the present study, a suitable method and appropriate conditions have been found for the spontaneous growth of millimeter-sized OH-free $\text{Ge}_{1-x}\text{Si}_x\text{O}_2$ single crystals with $0.5 \leq x \leq 0.93$. The new compositions reported here for high-quality flux-grown crystals having the

non-centrosymmetric α -quartz trigonal structure lead to provide, for the first time, a complete assessment of the $\text{GeO}_2\text{-SiO}_2$ solid solution. The silicon fraction was determined using the linear relationship established for the inter-tetrahedral bridging angle. Except for the bridging $T\text{-O-T}$ angle, the main structural parameters such as cell dimensions, characteristic bonds and angles deviate from the Vegard law when germanium is gradually replaced by silicon, in conjunction with a higher distortion of the α -quartz GeO_2 compared to the more regular $\alpha\text{-SiO}_2$ structure. The existence of a complete and continuous solid solution $\alpha\text{-GeO}_2\text{-}\alpha\text{-SiO}_2$ suggests that piezoelectric, optic, elastic, and mechanical properties are readily tunable by adjusting the Si and Ge contents at the mixed atomic site.

Acknowledgments

The financial and infrastructure support of the University of Montpellier is gratefully acknowledged. The single-crystal X-ray diffraction experiments were done using the technological resources of the X-ray and gamma-ray network at the University of Montpellier, France.

References

- [1] Piezoelectric, elastic, structural, and dielectric properties of the $\text{Si}_{1-x}\text{Ge}_x\text{O}_2$ solid solution: a theoretical study
KE El-Kelany, A Erba, P Carbonnière, M Rérat
Journal of Physics: Condensed Matter 26 (20) (2013) 205401

- [2] The composition, unit cell parameters, and microstructure of quartz during phase transformation from α to β as examined by in-situ high-temperature X-ray powder diffraction
Kohobhange S.P. Karunadasa, C.H. Manoratne, H.M.T.G.A.Pitawala, R.M.G.Rajapak
J. Physics and Chemistry of Solids, 119 (2018) 315
[10.1016/j.jpcs.2018.02.028](https://doi.org/10.1016/j.jpcs.2018.02.028)

- [3] Quartz: structural and thermodynamic analyses across the α - β transition with origin of negative thermal expansion (NTE) in β quartz and calcite.
M. Antao
Acta Cryst. B72, (2016) 249–262

- [4] Hydrothermal Crystal Growth of Piezoelectric α -Quartz Phase of AO_2 ($A = \text{Ge, Si}$) and MXO_4 ($M = \text{Al, Ga, Fe}$ and $X = \text{P, As}$): A Historical Overview.
O. Cambon, J. Haines
Crystals 7(2) (2017) 38
[10.3390/cryst7020038](https://doi.org/10.3390/cryst7020038)
- [5] Flux-Grown Piezoelectric Materials: Application to α -Quartz Analogues
P. Armand, A. Lignie, M. Beaurain, P. Papet
Crystals 4(2) (2014) 168-189
[10.3390/cryst4020168](https://doi.org/10.3390/cryst4020168)
- [6] Vibrational origin of the thermal stability in the highly distorted α -quartz-type material GeO_2 , an experimental and theoretical study.
G. Fraysse, A. Lignie, P. Hermet, P. Armand, D. Bourgoigne, J. Haines, B. Ménaert, P. Papet,
Inorg. Chem. 52 (2013) 7271-7279.
- [7] High-temperature piezoelectric properties of flux-grown α - GeO_2 single crystal
Ph. Papet, M. Bah, A. Haidoux, B. Rufflé, B. Menaert, A. Peña, J. Debray, P. Armand
J. Appl. Phys. 126 (2019) 144102.
[10.1063/1.5116026](https://doi.org/10.1063/1.5116026)
- [8] High-Temperature Elastic Moduli of Flux-Grown α - GeO_2 Single Crystal
A. Lignie, W. Zhou, P. Armand, B. Rufflé, R. Mayet, J. Debray, P. Hermet, B. Ménaert, P. Thomas, P. Papet
ChemPhysChem, 15 (2014) 118-125.
- [9] Growth and Characterization of GeO_2 single crystals with the quartz structure.
D.V. Balitsky, V.S. Valitsky, D.Y. Pushcharovsky, G.V. Bondarenko, A.V. Kosenko.
J. Crystal Growth, 180 (1997) 212-219.
- [10] Top-Seeded Solution Growth and Structural Characterizations of α -quartz-like Structure GeO_2 Single Crystal.
A. Lignie, B. Ménaert, P. Armand, A. Peña, J. Debray, P. Papet
Cryst. Growth Des. 13 (2013) 4220-4225.
- [11] Modulation of quartz-like GeO_2 structure by Si substitution: an X-ray diffraction study of $\text{Ge}_{1-x}\text{Si}_x\text{O}_2$ ($0 \leq x < 0.2$) flux-grown single crystals.
A. Lignie, D. Granier, P. Armand, J. Haines, P. Papet
J. Appl. Cryst. 45 (2012) 272-278.
- [12] Growth of piezoelectric water-free GeO_2 and SiO_2 -substituted GeO_2 single crystals,
A. Lignie, P. Armand, P. Papet.
Inorg. Chem. 50 (2011) 9311-9317.
- [13] Hydrothermal Growth and Structural Studies of $\text{Si}_{1-x}\text{Ge}_x\text{O}_2$ Single Crystals
V. Ranieri, S. Darracq, M. Cambon, J. Haines, O. Cambon, A. Largeteau, G. Demazeau
Inorg. Chem. 50, 10 (2011) 4632-4639
- [14] In Situ X-ray Absorption Spectroscopy Study of $\text{Si}_{1-x}\text{Ge}_x\text{O}_2$ Dissolution and Germanium Aqueous Speciation under Hydrothermal Conditions
V. Ranieri, J. Haines, O. Cambon, C. Levelut, R. Le Parc, M. Cambon, J.-L. Hazemann
Inorg. Chem. 51, 1 (2012) 414-419
- [15] Piezoelectric and non-linear optical properties of α -quartz type $\text{Si}_{1-x}\text{Ge}_x\text{O}_2$ single crystals

D. Clavier, M. Prakasam, A. Largeteau, J. J. Boy, B. Hehlen, M. Cambon, P. Hermet, J. Haines, O. Cambon
CrystEngComm, 18 (2016) 2500-2508.

[16] CrysAlis'Red software package, Oxford diffraction Ltd, Abingdon, United Kingdom, 2004.

[17] Crystal structure refinement with *SHELXL*

G. M. Sheldrick

Acta Crystallogr. C71 (2015) 3-8

[10.1107/S2053229614024218](https://doi.org/10.1107/S2053229614024218)

[18] SHELXT - Integrated space-group and crystal-structure determination

G. M. Sheldrick

Acta Crystallogr. A71 (2015) 3-8

[10.1107/S2053273314026370](https://doi.org/10.1107/S2053273314026370)

[19] International Table for Crystallography,

A. J. C. Wilson

Volume C, Dodrecht: Kluwer Academic Publishers (1992).

[20] Structure TIDY - a computer program to standardize crystal structure data

L. M. Gelato, E. Parthé

J. Appl. Cryst. 20 (1987) 139–143.

[10.1107/S0021889887086965](https://doi.org/10.1107/S0021889887086965)

[21] <http://www.ccdc.cam.ac.uk/conts/retrieving.html>

(or from the CCDC, 12 Union Road, Cambridge CB2 1EZ, UK; Fax: +44 1223 336033; E-mail: deposit@ccdc.cam.ac.uk).